

Vibration Analysis of Rolling Element Bearings (Air Conditioning Motor Case Study)

Konstantinos Kamaras, Anastasios Garantziotis and Ilias Dimitrakopoulos
Email: cbm@fnt.gr

Abstract

Condition based maintenance (CBM) philosophy uses a variety of monitoring techniques in order to assess the necessity of repair actions prior to a system's defect occurring. The methods that can be used for machinery evaluation include techniques such as vibration analysis, thermography, acoustic emission, oil and wear particle analysis. The aforementioned techniques are a potential asset of any maintenance personnel that aims to reduce the life cycle cost of industrial equipment. The aim of this paper is to present an example of the application of vibration analysis as an efficient, cost-effective and reliable maintenance technique for motor bearings fault diagnosis.

Keywords

Vibration Analysis, Rolling Element Bearings, Fast Fourier Transform, Envelope Analysis.

1. Introduction

Any rotating machinery produces a vibration signature that is strongly related with system performance and condition. Any potential fault will amplify vibration signal's energy or even distort the vibration waveform and spectrum. The most common faults of industrial equipment can be identified at early stages as they usually distort the machinery's vibration signature. Therefore, vibration analysis can at an early stage pinpoint issues such as unbalance and misalignment which are the main cause of industrial equipment defects. Not only the aforementioned faults, but also worn gears or bearings, bent shafts, rotor rubs, system looseness (structural or rotating), belt transmission problems, resonance and electromagnetic issues can be identified using vibration signal signature.

Taking into account that rolling element bearings (REB) are major components of any rotating equipment, a timely bearing defect identification has substantial importance. Albrecht et. al (1986) research showed that about 41% of catastrophic failures in motors are related with bearing components. Different digital signal processing (DSP) techniques can be used in vibration analysis for REB fault diagnosis. These methods include frequency or time- frequency domain algorithms. Even the time waveform under some conditions can be exploited in vibration analysis. Very useful techniques such as discrete wavelet transform (DWT), continuous wavelet transform (CWT), Hilbert - Huang transform (HHT) have been tested in experimental level. However, Discrete Fourier Transform (DFT)

remains the most familiar DSP tool in vibration analysis as it can produce very effective and reliable results in vibration monitoring.

REB fault recognition is based on the detection of some characteristic frequencies which are property of the bearing geometry, rotational speed and number of rolling elements. A bearing under normal working condition should not produce its Characteristic Defect Frequencies (CDF) at the vibration spectrum. However, any potential fault at bearing races, rolling elements or cage usually generate the CDF that can be calculated based on the formulas tabulated in **Table 1**. It should be noted that the results from the equations of table 1 do not assume slippage phenomenon and therefore the estimated CDF can vary by 1-2 % (Smith and Randall, 2015). Furthermore, one property of bearing's CDF is that are not integer multiples of shaft rotational speed. This characteristic allows us to suspect a potential bearing problem even if its type is unknown.

The paper is organized as follows: Section 2 summarizes the theoretical background of bearing fault stages and envelope analysis. Section 3 presents an application example of bearing fault detection in a motor using vibration analysis. In this section, spectral kurtosis technique is also tested as an early estimator. Finally, the conclusions of the bearing defect are discussed in section 4.

Ball Pass Frequency Outer Race (BPFO)	$f_s \cdot N_b / 2 \cdot (1 - B_d \cdot \cos \varphi / P_d)$	Inner/ Outer race rotation
Ball Pass Frequency Inner Race (BPFI)	$f_s \cdot N_b / 2 \cdot (1 + B_d \cdot \cos \varphi / P_d)$	Inner/ Outer race rotation
Ball Spin Frequency (BSF)	$f_s \cdot (P_d / 2 \cdot B_d) \cdot (1 + B_d^2 \cdot \cos^2 \varphi / P_d^2)$	Inner/ Outer race rotation
Fundamental Train Frequency (FTF)	$f_s \cdot 1/2 \cdot (1 - B_d \cdot \cos \varphi / P_d)$	Inner race rotation
	$f_s \cdot 1/2 \cdot (1 + B_d \cdot \cos \varphi / P_d)$	Outer race rotation

Table 1. Bearing fault frequencies (f_s , N_b , B_b , P_d and φ are the rotating frequency, the number of balls, the ball diameter, the pitch diameter and the contact angle respectively) (Taylor and Kirkland, 2004).

2. Bearing Failure Stages

A bearing fault usually develops in different stages and consequently that affects the diagnosis procedure. At vibration monitoring a bearing defect can be categorized in four stages of wear depending on the size of defect and the patterns they produce at the frequency spectrum. At the first stage, a bearing defect would not cause any abnormal noise or temperature deviation and can be identified only by techniques that work efficiently at high frequency regions (20 to 40 kHz). In general, the high frequency techniques take advantage of bearing's natural frequency (envelope spectrum) excitation or use transducers with known resonant frequency (Shock Pulse Method- SPM). High frequency techniques due to their sensitivity can be used for early warning, confirmation and localization of a bearing defect (especially for low speed machines). It is recommended that maintenance personnel should not proceed directly to a high-speed machine overhaul until signs of wear could be identified in lower frequency region as the defect size at this stage will remain at microscopic level. At this stage bearing lubrication and condition monitoring is advisable.

As the defect develops the bearing enters the second stage of fault. In that case high energy impacts will excite bearing natural frequency and high frequency (1 to 5 kHz) energy level

starts to increase. In this case high frequency demodulation (envelope analysis) and acceleration (high frequency) spectrum can pinpoint the bearing fault whereas low frequency (velocity) spectrum will still not show any evidence of wear.

Envelope analysis is based on the observation that bearing fault impulses are amplified by the resonance of the structure that supports the bearing or the bearing itself thus yielding a high signal to noise ratio. It is a three-stage procedure which is depicted in **Figure 1**. It involves the band-pass filtering of the raw vibration signal in a high frequency region where the fault impacts are amplified by structural resonances (Randal and Antoni, 2011). Then the signal is rectified and amplitude demodulated using an envelope detector such as the Hilbert transform. Finally, the spectrum of the envelope signal is calculated using FFT algorithm which usually can display the characteristic bearing defect frequencies at low frequency region efficiently. Typical patterns of the envelope signals of a bearing with outer race or inner race fault are depicted in **Figure 2**. Envelope analysis have been proven very efficient at detecting bearing faults or lack of lubrication at early stages.

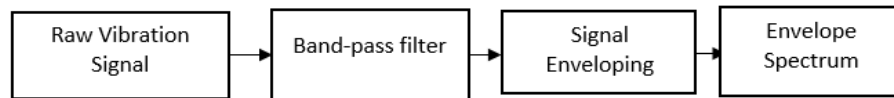


Figure 1. Process of envelope analysis.

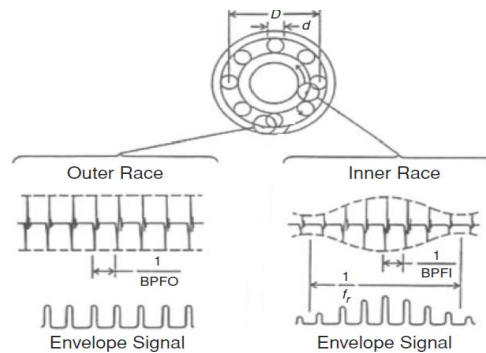


Figure 2. Envelope signals for outer or inner race bearing faults (Randall, 2011).

At the third stage of a bearing fault the most commonly recognizable patterns can be measured at low frequency spectrum. Despite the fact that high frequency energy continues to increase and envelope analysis is still efficient, the classic patterns of bearing failure are now present at velocity spectrum. On the one hand, for outer race fault harmonics of BPFO should be measured at low frequency spectrum. On the other hand, in the case of inner race fault harmonics of BPF_I with shaft rotational speed sidebands would appear. The sidebands around the BPF_I are present because as the inner race defect passes through the load zone it creates amplitude modulated vibration signal. All the aforementioned patterns are valid for inner race rotation, while when the outer race rotates the patterns of BPFO and BPF_I fault are reversed. Ball or roller defects generate BSF or multiples of it with FTF sidebands

at velocity spectrum. Usually the presence of three harmonics is enough in order to decide a bearing replacement as soon as possible.

At the final stage of a bearing wear significant damage is present and the patterns described before would change. Specifically, the vibration spectrum noise floor will start to raise and the CDF will start to disappear. The vibration pattern now starts being similar to rotating looseness fault condition (integer multiples of running speed). Also, vibration periodicity is not present due to the damage extension thus producing multiple harmonics of shaft rotational speed. Machines with bearings having stage 4 vibration patterns should not be operated as a catastrophic failure can be imminent.

3. Motor Bearing Fault Diagnosis

The machine of interest was the motor of a ship's air conditioning system that is composed of three coupling connected motors and compressors. The No 4 air conditioning machine was found with a motor d.e. bearing issue. The motor, which is depicted in **Figure 3**, is 105 kW, 1770 rpm and it has a NU316 Drive End (DE) and a 6316 Non Drive End (NDE) bearing respectively. The failure was diagnosed at the DE bearing (NU316- Koyo) using vibration analysis. The Digivibe MX9 vibration analysis software and a 100 mV accelerometer were used. The sampling frequency was 44.1 kHz and the diagnosis was based on FFT algorithm and envelope analysis. The measurements were carried out at motor d.e. and n.d.e., motor and compressor mounting bolts and compressor, compressor d.e. and n.d.e., compressor cylinder valves and frame in horizontal, vertical and axial directions.



Figure 3. Motor and compressor of ship's air conditioning system. The location of motor d.e. bearing is highlighted.

Prior to the vibration analysis measurements, it was noticed that the motor had an increased temperature at motor d.e. The maintenance personnel reported that motor bearings were replaced six months ago and were lubricated according to the manufacturer's guidelines. However, the vibration analysis showed a motor d.e. defect and the maintenance department was advised to replace the bearing as soon as possible.

The vibration analysis low frequency (velocity) waveform and spectrums at motor d.e. in horizontal direction are depicted in **Figure 4**. As it can be observed apart from the high level of the fundamental frequency of 29.6 Hz (1X) that corresponds to motor running speed there is also a non- integer multiple frequency component of it 160.5 Hz (5.42X) which is related to motor d.e. bearing (NU316) CDF of BPFO. Harmonics of BPFO start

to emerge in the frequency spectrum which shows that the bearing failure is in a developed stage. The aforementioned harmonics are better recognizable in dB as it can be observed at **Figure 4** (bottom graph). Finally, sidebands of motor running speed were measured around BPFO thus showing modulation.

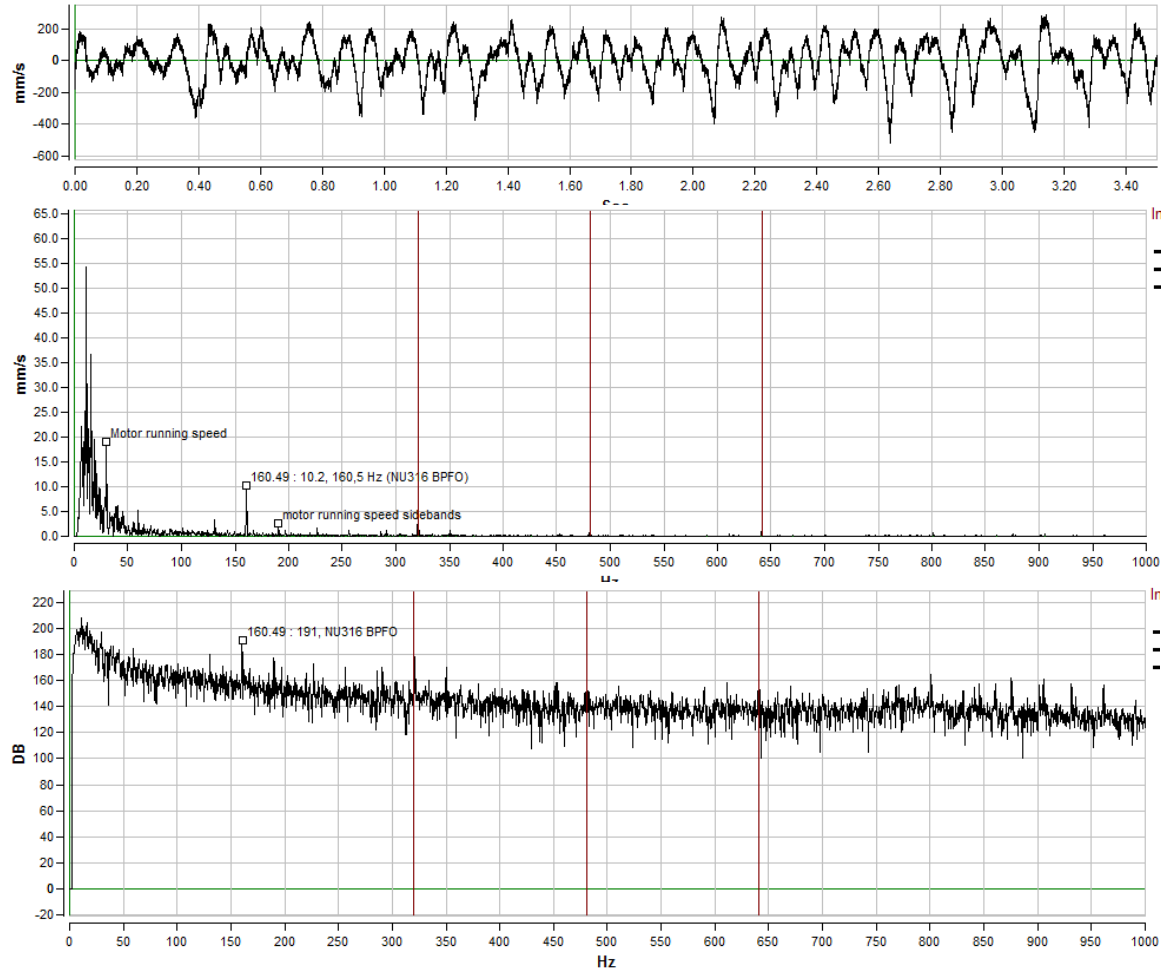


Figure 5. Motor d.e. velocity waveform (top), velocity spectrum in linear scale (middle) and in dB (bottom) respectively.

Furthermore, the high frequency (acceleration) waveform and spectrum at motor d.e. are depicted in **Figure 5**. The acceleration waveform apart from the increased energy level it is also truncated which indicates movement restriction. Additionally, the acceleration spectrum has the 5.42X frequency component with harmonics and high frequency components at the region of 1.5-2.5 kHz which correspond to bearing or structure resonant frequencies. The excitation of these frequencies can be justified by the bearing impacts occurring due to a defect at its races as the distance between the frequency peaks corresponds to the NU316 BPFO. This phenomenon can be observed clearly at the lower image, where the distance between high frequency peaks is highlighted and equals to motor d.e. bearing BPFO.

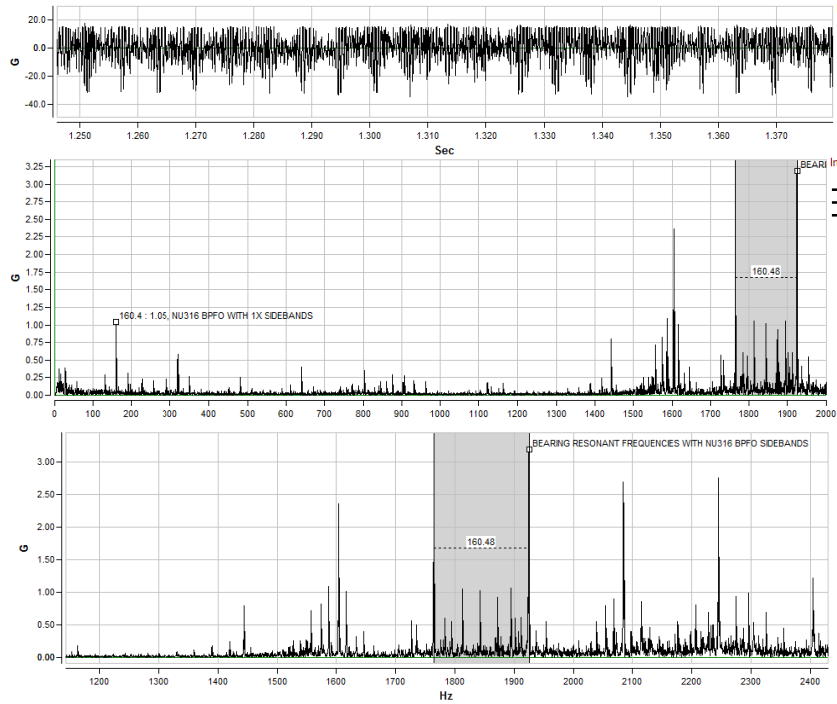


Figure 5. Motor d.e. acceleration spectrum (top) and zoomed spectrum at band of 1-2.5 kHz (bottom).

The vibration data at motor d.e. were further analyzed using envelope analysis. The results showed that the frequency component of 160.5 Hz (NU316 BPFO) and its higher order harmonics are present at demodulated spectrum. Furthermore, an attenuated frequency component of 226.8 Hz (NU316 BPF1) with motor running speed sidebands was measured. The demodulated spectrums of envelope analysis in horizontal and vertical directions of motor d.e. are shown in **Figure 6**. Although the existence of bearing CDF at demodulated spectrum can be caused due to improper lubrication, the high acceleration energy (9.5 g RMS- 48 g pk-pk) of the waveform and the aforementioned velocity spectrums indicate extensive bearing wear. Envelope analysis verifies that there is a motor d.e. bearing issue.

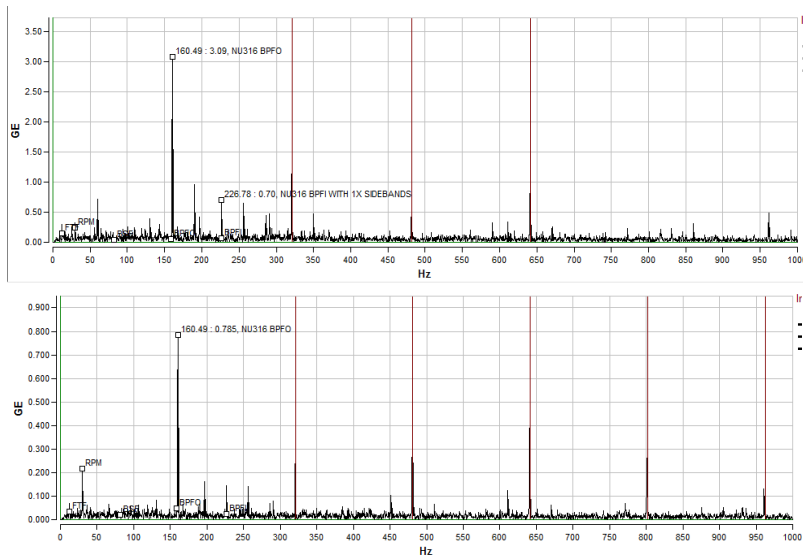
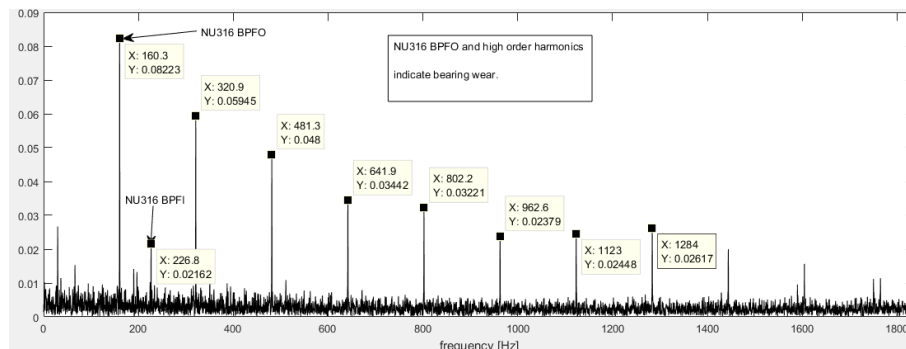


Figure 6. Motor d.e. demodulated spectrum in horizontal (top) and vertical (bottom) directions.

The same data was also analyzed using the method of spectral kurtosis in order to select the band pass filter prior to the demodulation process of envelope analysis. This post processing method allows the selection of the filter based on the value of kurtosis. In general, a bearing defect causes kurtosis to increase and therefore filtering the data at the frequency band that has increased value of kurtosis (most impulsive frequency band) enhances the bearing fault detection ability.

Using the method of spectral kurtosis prior the envelope analysis the results showed much more clearly the bearing fault. The fast kurtogram algorithm of Antoni (2007) was used in Matlab software in order to find the most impulsive frequency band prior to the band pass filtering. The demodulated spectrums in **Figure 7** show the presence of NU316 BPFO (160.5 Hz) and its higher order harmonics much clearly. The presence of motor running speed sidebands around the BPFO should also be noted at the demodulated spectrum. The aforementioned pattern indicates amplitude modulation. This phenomenon can be observed at the vibration data taken in the vertical direction of **Figure 7**. Furthermore, there is a frequency component (226.8 Hz) which corresponds to NU316 BPFI, but still there are not its high order harmonics present.

The results of vibration analysis showed the necessity of motor d.e. bearing replacement. In general, when the CDF are present at velocity spectrum and the time waveform has high energy impacting (high periodic impacts) the defective bearing is recommended to be replaced. Indeed, the results after NU316 bearing replacement show significant damage at both races (inner and outer race) and no wear at rolling elements as it can be observed in **Figure 8**. The symptom is more intense at the bearing inner race but there are not harmonics of this CDF. This can be explained from the fact that high frequency energy is severely affected by the distance of the point where the accelerometer is mounted (measurement point). This distance is also known as the signal transmission path, which has a tremendous effect on high frequency components. This is due to the fact that high frequencies are attenuated by the distance from the source of vibration to the accelerometer mounting position thus causing the high frequency information to get masked by other vibration sources. Therefore, as bearing defects initially appear in high frequency regions the improper transmission path may mask this valuable information. Furthermore, it should be noticed that the tracks created on both races are equally spaced and sized and located at the bearing load zone. It was found that they were created due to the contact of the rolling elements cage with the bearing races.



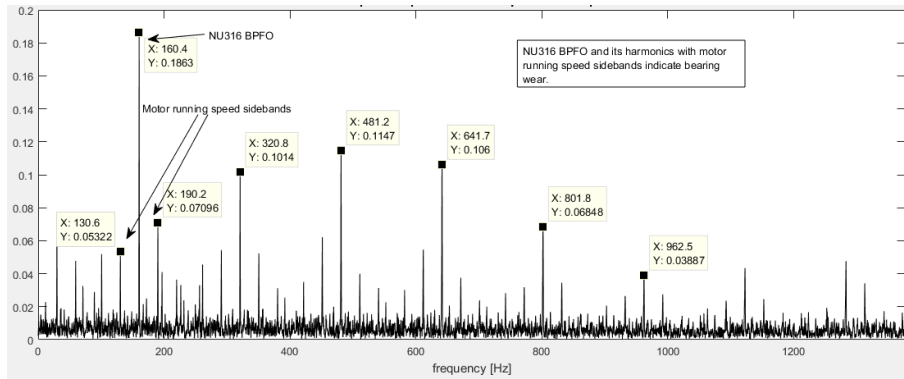


Figure 7. Motor d.e. demodulated spectrum in horizontal (top) and vertical (bottom) directions using band pass filter based on kurtosis values. The components of CDF are noted.



Figure 8. Motor d.e. bearing NU316 in good condition prior the replacement (top left), bearing outer race (top right), bearing inner race (bottom left) and rolling elements (bottom right).

After the bearing replacement, the vibration measurements were repeated showing the absence of bearing CDF and significant energy decrease in the high frequency region. Also, envelope analysis did not show any symptoms of lack of lubrication as no frequency components of CDF were measured. The vibration data are shown in **Figure 9**.

First of all, the waveform has low RMS, pk-pk, kurtosis and crest factor values and no signs of bearing impacting. Additionally, the zoomed acceleration spectrum (figure 9 middle graph) does not contain any frequency component related to bearing CDF. Finally, the acceleration spectrum does not have energy concentration at high frequency region (over 1 kHz) and there is no bearing or structure resonant frequencies excitation. The frequency peak at 1718 Hz is not related with any bearing impacting or resonant frequency excitation but with the rotor bar frequency which is a typical pattern for electric motors. Therefore the vibration spectrum verifies that the motor d.e. bearing is in good condition.

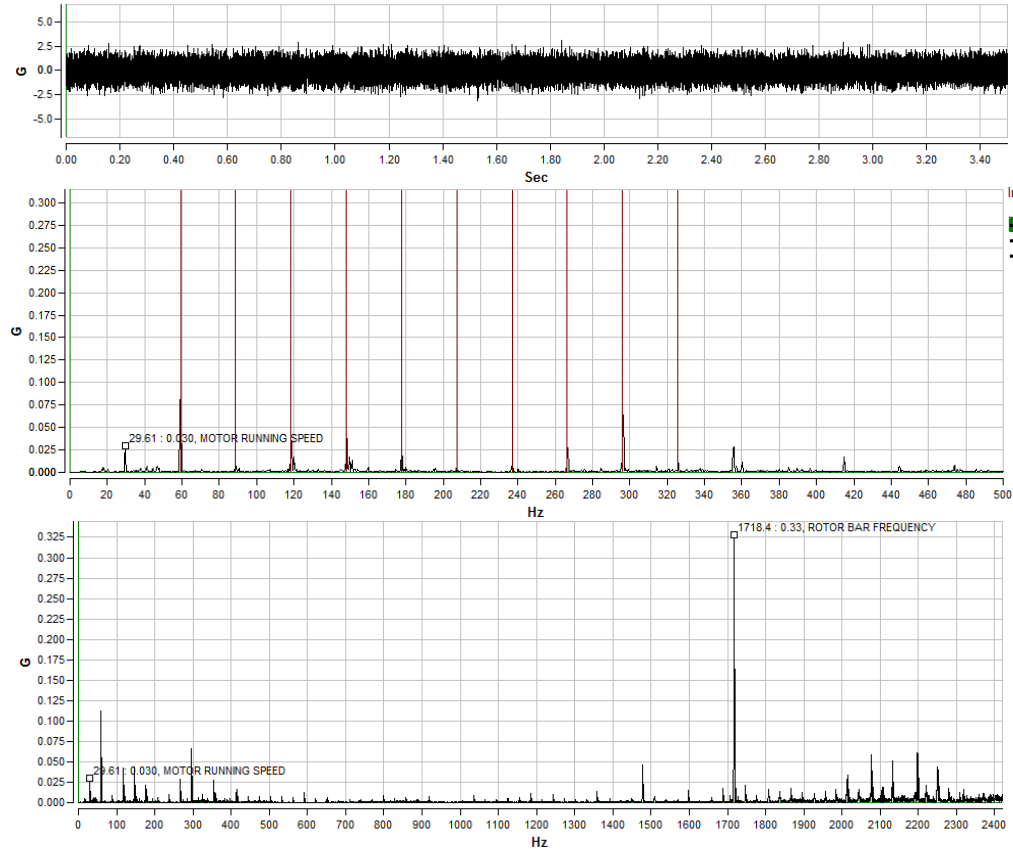


Figure 9. Motor d.e. acceleration waveform (top), zoomed at 0-500 Hz acceleration spectrum (middle) and 0-2.5 kHz acceleration spectrum (bottom).

4. Conclusion

In this application note the effectiveness of vibration analysis in bearings fault detection was presented. Frequency analysis, via the adequate algorithms, of the vibration signal pinpointed the bearing fault providing the maintenance department the early warning of an imminent motor bearing failure. The combination of FFT algorithm and envelope analysis have been proven to be very efficient and reliable signal processing techniques in vibration monitoring and specifically in bearing fault diagnosis. Considering the wide range of bearings application in maritime industry the adoption of vibration analysis, which is a non-intrusive technique, in a prediction based maintenance program can decrease equipment downtime, reduce unnecessary inspections, enhance maintenance department schedule and offer time for spare part finding.

7.0 References

Albrecht P.F., Appiarius J.C., McCoy R.M., Owen E.L., Sharma D.K. (1986) "Assessment of the Reliability of Motors in Utility Applications – Updated" IEEE Energy Conversion, Available at:

<http://ieeexplore.ieee.org/stamp/stamp.jsp?tp=&arnumber=4765668>

Antoni J. (2007), "Fast computation of the kurtogram for the detection of transient faults", Mechanical Systems and Signal Processing, Science Direct, Available at:

<http://www.sciencedirect.com/science/article/pii/S0888327005002414>

Smith W.A., Randall R.B. (2015), "Rolling Element Bearing Diagnostics Using the Case Western Reserve University Data: A Benchmark Study", Science Direct, Mechanical Systems and Signal Processing, Available at: <http://www.sciencedirect.com/science/article/pii/S0888327015002034>

Randall R.B., Antoni J. (2011), "Rolling Element Bearing Diagnostics: a Tutorial", Science Direct, Mechanical Systems and Signal Processing, Available at:

<http://www.sciencedirect.com/science/article/pii/S0888327010002530>

Taylor J.I., Kirkland W. (2004) "The Bearing Analysis Handbook", Vibration Consultants, ISBN: 0-9640517-3-7, pp. 18-32.